FERMILAB-CONF-76-170-E #33

PRODUCTION OF CONTINUUM MUON PAIRS AT 225 GEV BY PIONS AND PROTONS*

K. J. Anderson, G. G. Henry, K. T. McDonald†, C. Newman, J. E. Pilcher‡,
E. I. Rosenberg
Enrico Fermi Institute, University of Chicago
Chicago, Illinois 60637

J. G. Branson, G. E. Hogan‡, R. D. Pisarski, G. H. Sanders, A. J. S. Smith,
J. J. Thaler
Joseph Henry Laboratories, Princeton University
Princeton, New Jersey 08540

(Submitted to XVIII Conference in High Energy Physics, Tbilisi, USSR, 1976)

ABSTRACT

We give preliminary results for the production of non-resonant continuum muon pairs in collisions of 225 GeV/c π^+, π^- and protons with carbon, and of 225 GeV/c π^+ and protons with tin. A comparison is made of the production of massive muon pairs by π^+ and π^- on carbon, an isoscalar target. Cross-section ratios and dependence of the cross-sections upon $M_{\mu\mu}$, x_F, p_T, and $\cos\theta^*$ are given. Some features of the continuum are compared to the pairs observed in the region of the resonances ρ, ω, ϕ and J.

As part of our study of muon pairs produced by hadrons on nuclear targets, we present preliminary results for non-resonant or continuum dimuons. Additional contributions to this Conference[1,2,3,4] discuss other aspects of the experiment, including a description of the detector[3] and the data analysis.

The data presented here represent an exposure of Carbon and Tin targets to π^+, π^- and protons.

Figures 1a and 1b show the mass spectra for all combinations of particle type and target measured. The spectra are similar in shape, display the known resonances and show a statistically useful sample below the J, and a smaller mumber of high mass continuum events above the J.

Many models[5,6,7] predict the formation of muon pairs by the annihilation of quarks and antiquarks in the target and projectile. For all previous experiments, where neutron or proton beams were used, all the antiquarks are provided by the sea, leading to rather model-dependent predictions for the features of the resulting spectrum. This is the first experiment to use π^+ and π^- beams on an isoscalar target, a particularly attractive experimental situation, in that valence antiquarks are present in the beam. Annihilations of fractionally charged valence quarks in the target with the antiquark in the projectile should then show a charge asymmetry

$$\frac{\sigma(\pi^+C)}{\sigma(\pi^-C)} = 1/4,$$

independent of details of the model. Unfortunately this large asymmetry is diluted by the presence of the isospin-symmetric quark-pairs in the sea. Using recent measurements of structure functions, Altarelli, Brandt, and Cabibbo[6], and Farrar[7] have estimated the effect of the sea, finding the charge ratio to be close to 1 at low pair masses, and then to decrease slowly to the

value 1/4 as M^2/s increases. For example, in the highest mass region for which we have adequate statistics, $M_{\mu\mu} \gtrsim 2.5$ GeV, the ratio is predicted to be ~ 0.6.

In four mass intervals below the J, and two at higher masses, we compare the production of dimuons by π^+ and p and by π^+ and π^- on Carbon. Figures 2a and 2b show these cross-section ratios and equivalent ratios for the J mass region. Of particular interest is the π^+/π^- ratio, which appears to change from approximately unity at low mass to about .25 at the highest masses, except for the J-mass region, where it returns, within errors, to unity. Within the limited statistics, this behavior is in agreement with the predictions of parton models.

When π^+ and proton induced pairs are compared, on the other hand (Fig. 2a) the J and continuum regions do not show any difference. In both Figures 2a and 2b the ρ_o-ω and ϕ mass regions are also shown, where a charge ratio of 1 is expected from isospin conservation.

Other features of the data have been studied in a preliminary manner by selecting three mass regions having significant numbers of events, in a region relatively free of resonance signal. The regions are: 1.5-1.9 GeV/c^2, 1.9-2.3 GeV/c^2, and 2.3-2.7 GeV/c^2.

Figure 3 shows the dependence of the cross-section in these bins on the variable $x_F \simeq \frac{2p_{//}}{\sqrt{s}}$, for p, π^+, and π^- incident on carbon. The basic feature of all these distributions, that the π-induced events have a slower fall-off with increasing x_F than those of p-induced events, is very similar to what we have observed in production of the resonances ρ, ω, ϕ, and J. [1] The data have been fitted to the form $B \cdot d\sigma/dx_F = A\ (1 - x_F)^b$; the best fits, of somewhat limited statistical significance, are summarized in Table 1 a.

Figure 4 illustrates the dependence of the differential cross-sections $d\sigma/dp_T^2$ upon the transverse momentum p_T of the dimuon. Exponentials both linear and quadratic in p_T^2 have been fit to these spectra, the results appearing in Table 1 b. The quadratic fits are shown in the figure, although either hypothesis gives an adequate fit. The slopes of these distributions do not differ significantly from that of J - production. This feature is seen in a simple way in Fig. 5, where we have plotted the average transverse momentum $< p_T >$ as a function of the dimuon mass, for π^+ and p- induced events. (The analysis of the π^- sample is not yet completed.) No difference is apparent between the production of resonant and non-resonant dimuons. Instead, one sees a slow, smooth increase of $< p_T >$ with increasing dimuon mass.

In Fig. 6 are plotted the relative differential cross-sections as a function of $\cos\theta^*$, where θ^* is the polar angle in the rest frame of the decaying dimuon. While the statistics are limited, a polarization consistent with $1 + \cos^2\theta^*$ is suggested, especially in the 1.9 - 2.3 GeV/c^2 mass region.

Finally, as shown in Fig. 7, we have fitted the mass dependence of the cross-section, for the portion of the π^- - carbon sample with masses from 1.3 to 2.7 GeV/c^2, to the form $d\sigma/dM \propto M^{-n}$. We obtain the value $n = 5.3 \pm 0.5$, with $\chi^2 = 2$ per degree of freedom, in general agreement with parton models.

To conclude, we mention again that these are only preliminary results, presented at this time to illustrate the basic features of the data. The present sample is being analysed more completely, to include the data taken with a tin target, and to explore the low-mass region, where our results at 150 GeV show a substantial non-resonant contribution.[1] To explore further some of the interesting features of the higher mass dimuons, we have been approved to carry out another experiment with intensities more than an order

of magnitude higher than we have been able to obtain so far.

The authors wish to acknowledge the use of the muon spectrometer developed by the Chicago-Harvard-Oxford-Illinois group, which we have modified for this work.

REFERENCES

* This research was supported in part by the National Science Foundation, and by the Energy Research and Development Administration.

† Enrico Fermi Postdoctoral Fellow.

‡ A. P. Sloan Fellow.

‡ National Science Foundation Predoctoral Fellow.

1. K. J. Anderson et al., Inclusive μ-pair Production at 150 GeV by π^+ Mesons and Protons, Contribution to this Conference.

2. K. J. Anderson et al., The Contribution of Muon Pairs to the Yield of Single Prompt Muons, Contribution to this Conference.

3. K. J. Anderson et al., Production of the J(3.1) and ψ' (3.7) by 225-GeV π^+, π^-, and Protons, Contribution to this Conference.

4. K. J. Anderson et al., High-Sensitivity Search for Multi-Muon Events Produced by 225-GeV Hadrons, Contribution to this Conference.

5. S.D. Drell and T.M. Yan, Phys. Rev. Letters 25, 316 (1970).

6. G. Altarelli et al., Nuclear Physics B92, 413 (1975).

7. G. R. Farrar, Nuclear Physics B77, 426 (1974).

Table 1. Fits of Continuum Production Cross-Sections

$$\begin{pmatrix} p \\ \pi+ \\ \pi- \end{pmatrix} + C \rightarrow \mu^+\mu^- + X$$

Note: All cross-sections are per Carbon Nucleus.

a) Dependence on x_F: $B \cdot \frac{d\sigma}{dx_F} = A(1-x)^b$ nanobarns/nucleon

Beam	Mass Region	A	b	χ^2/dof
p	1.5-1.9	260±32	4.9±.3	3.4
	1.9-2.3	51±21	3.8±.7	.82
	2.3-2.7	45±11	5.2±.6	.86
π^+	1.5-1.9	321±92	3.5±.6	1.4
	1.9 2.3	34±18	1.7±.8	.88
	2.3-2.7	28±29	2.3±1.6	.63
π^-	1.5-1.9	170±78	2.5±.7	1.5
	1.9-2.3	52±23	2.4±.8	.16
	2.3 2.7	29±11	1.7±.7	1.7

b) Dependence on p_T: (units of $\frac{Bd\sigma}{dp_T^2}$ are nanobarns/(GeV/c^2)/nucleus)

		Linear $B\cdot d\sigma/dp_T^2 = Ce^{-dp_T}$			Quadratic $B\cdot d\sigma/dp_T = Fe^{-gp_T^2}$		
Beam	Mass Region	C	d	χ^2/dof	F	g	χ^2/dof
p	1.5-1.9	381±30	2.9±.1	3.9	84±4	1.2±.05	1.9
	1.9-2.3	110±33	3±.3	.75	24±3	1.3±.1	.55
	2.3-2.7	25±14	2.4±.5	.85	7.5±1.2	.98±.12	.75
π^+	1.5-1.9	586±106	3.3±.2	.88	110±11	1.4±.1	.3
	1.9-2.3	66±30	2.4±.5	.3	21±6	1.1±.25	.001
	2.3-2.7	89±60	3.5±.8	.44	17±6	1.7±.4	.5
π^-	1.5-1.9	269±60	2.7±.2	2.7	67±7	1.1±.1	1.1
	1.9-2.3	28±12	1.6±.4	1.2	13±3	.65±.15	.5
	2.3-2.7	32±18	2.0±.5	.5	11±3	.81±.18	.3

Table I (continued)

c. Dependence on $\cos\theta^*$: (Relative cross section) $d\sigma/d(\cos\theta^*) \propto (1 + \alpha \cos^2\theta^*)$

Beam	Mass Region	α	χ^2/dof
p	1.5-1.9	.66±.24	.38
	1.9-2.3	3.3±.9	.95
	2.3-2.7	-.09±.8	2.7
π^+	1.5-..9	.11±.35	1.5
	1.9-2.3	1.8±1.4	.37
	2.3-2.7	1.5±1.7	.43
π^-	1.5-1.9	.63±.54	1.2
	1.9-2.3	1.8±1.6	.35
	2.3-2.7	1.5±1.8	2.5

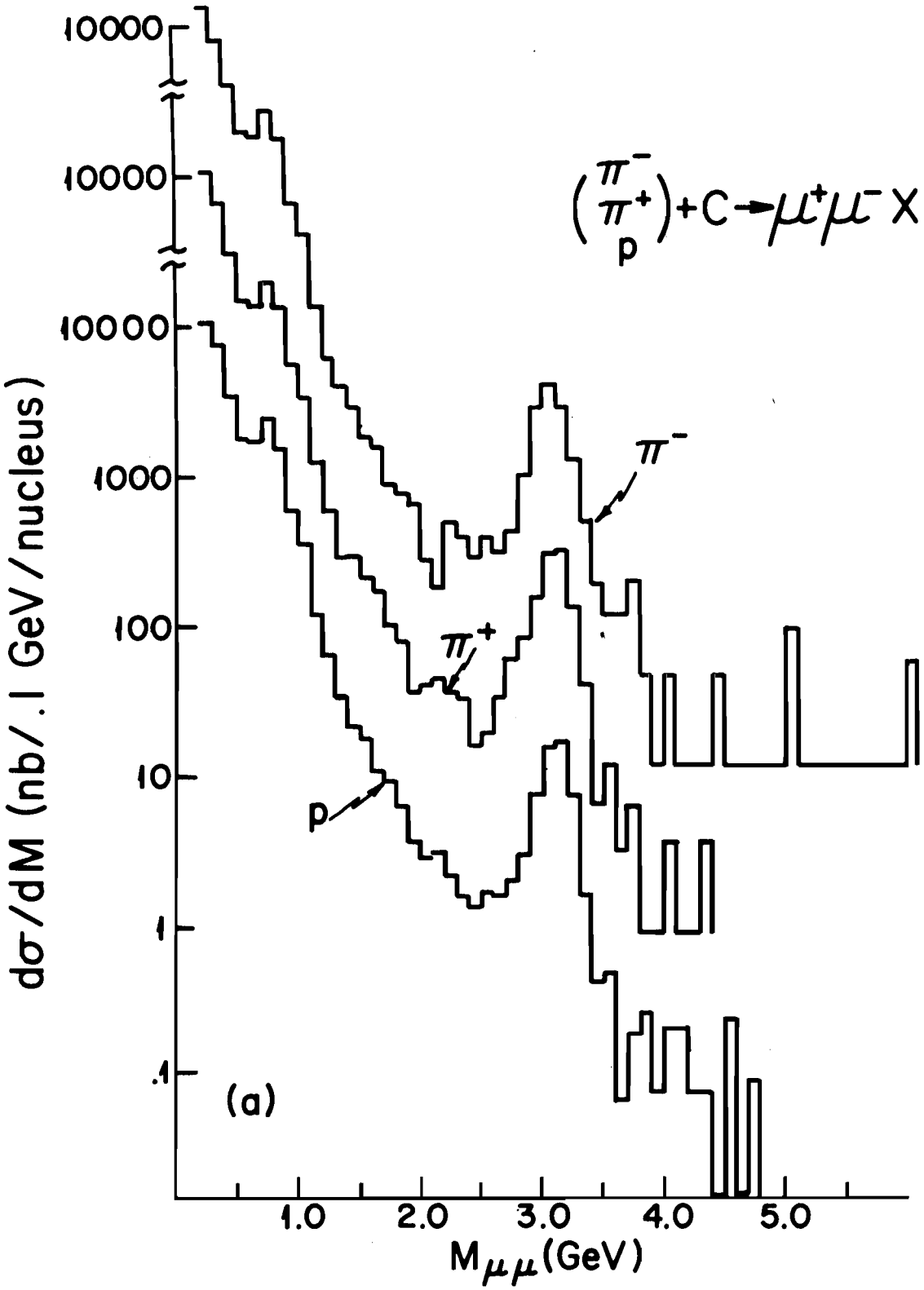
10000
10000
10000
1000
100
10
1
.1
dσ/dM (nb/.1 GeV/nucleus)
$\binom{\pi^-}{\pi^+}_p$ + C → μ⁺μ⁻ X
π⁻
π⁺
p
(a)
1.0
2.0
3.0
4.0
5.0
Mμμ(GeV)

FIGURE 1 a

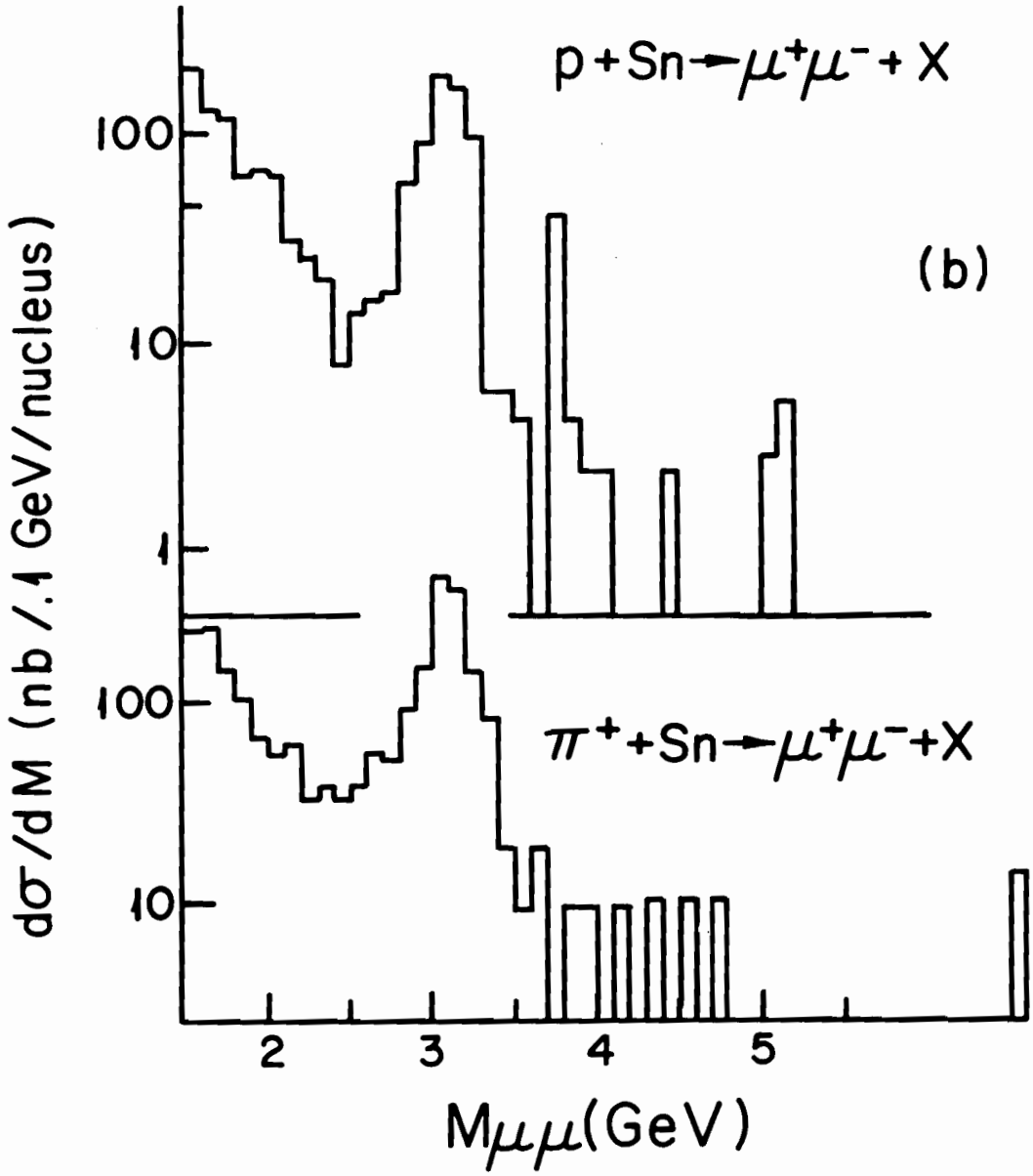
p+Sn→μ⁺μ⁻+X
(b)
π⁺+Sn→μ⁺μ⁻+X
100
10
1
100
10
2
3
4
5
dσ/dM (nb/.1 GeV/nucleus)
Mμμ(GeV)

FIGURE 1 b

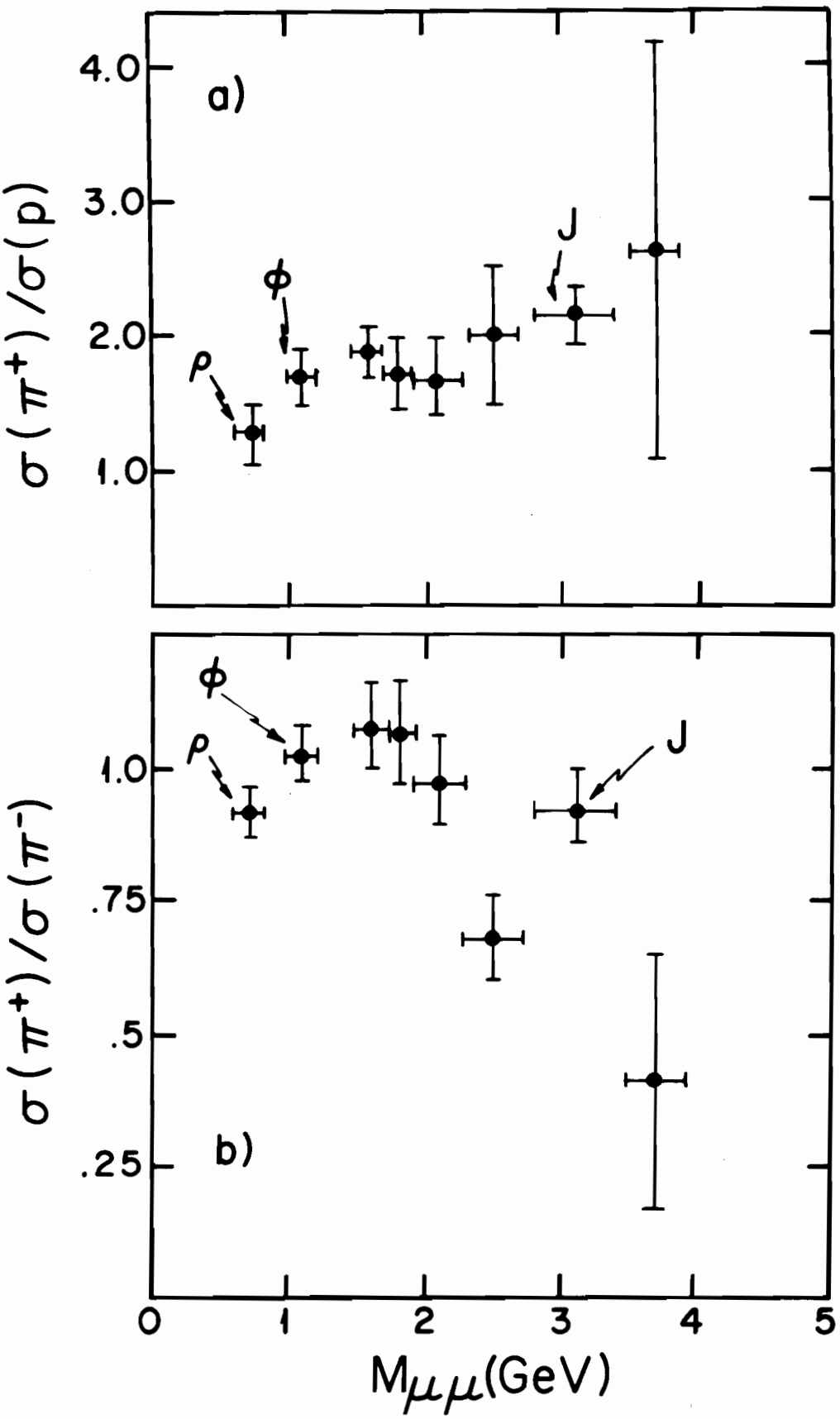

FIGURE 2

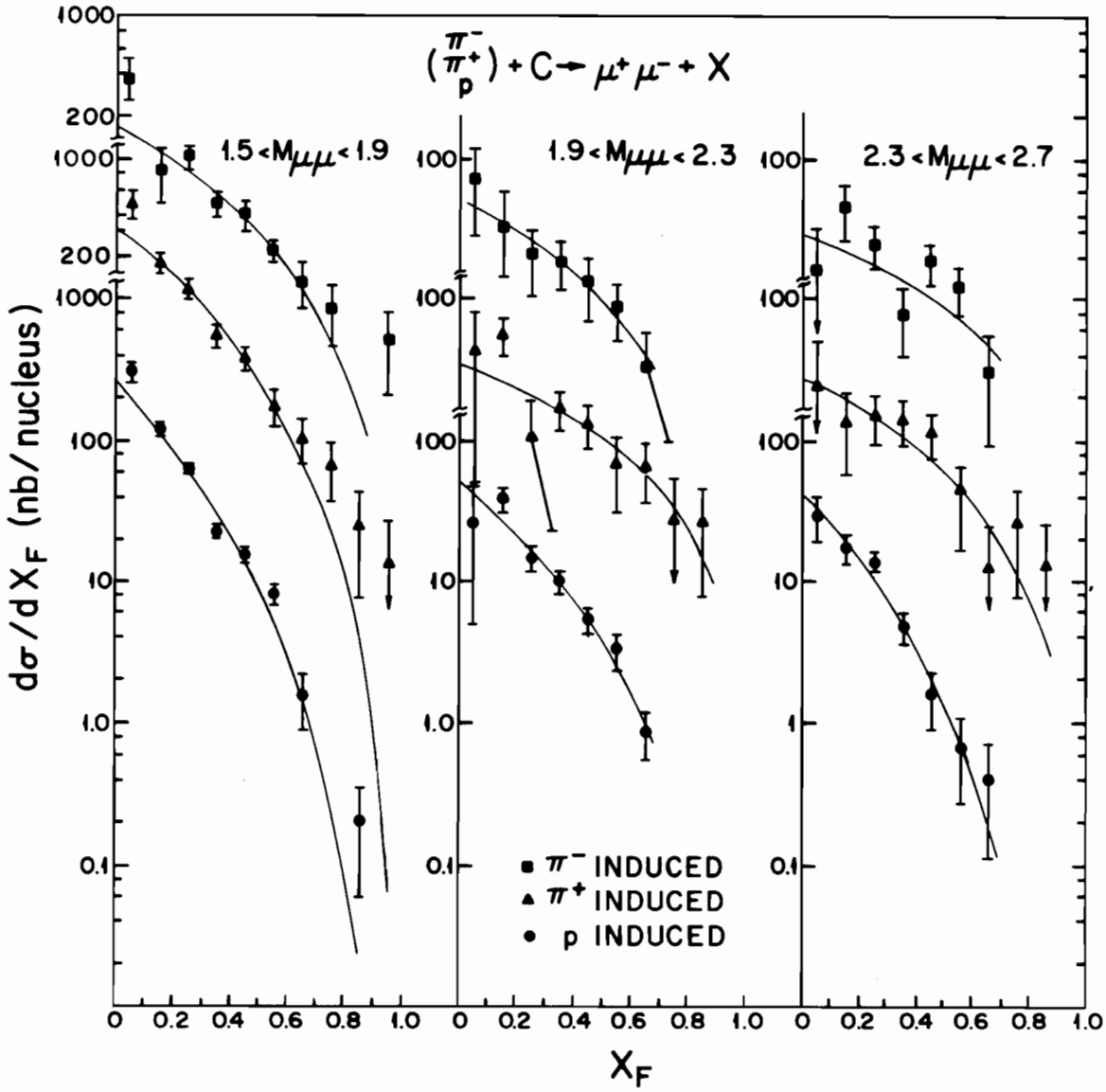
$(\pi^-_{p}\ \pi^+)$ + C → $\mu^+\mu^-$ + X
1.5 < Mμμ < 1.9
1.9 < Mμμ < 2.3
2.3 < Mμμ < 2.7
dσ/d X_F (nb/nucleus)
X_F
π⁻ INDUCED
π⁺ INDUCED
p INDUCED

FIGURE 3

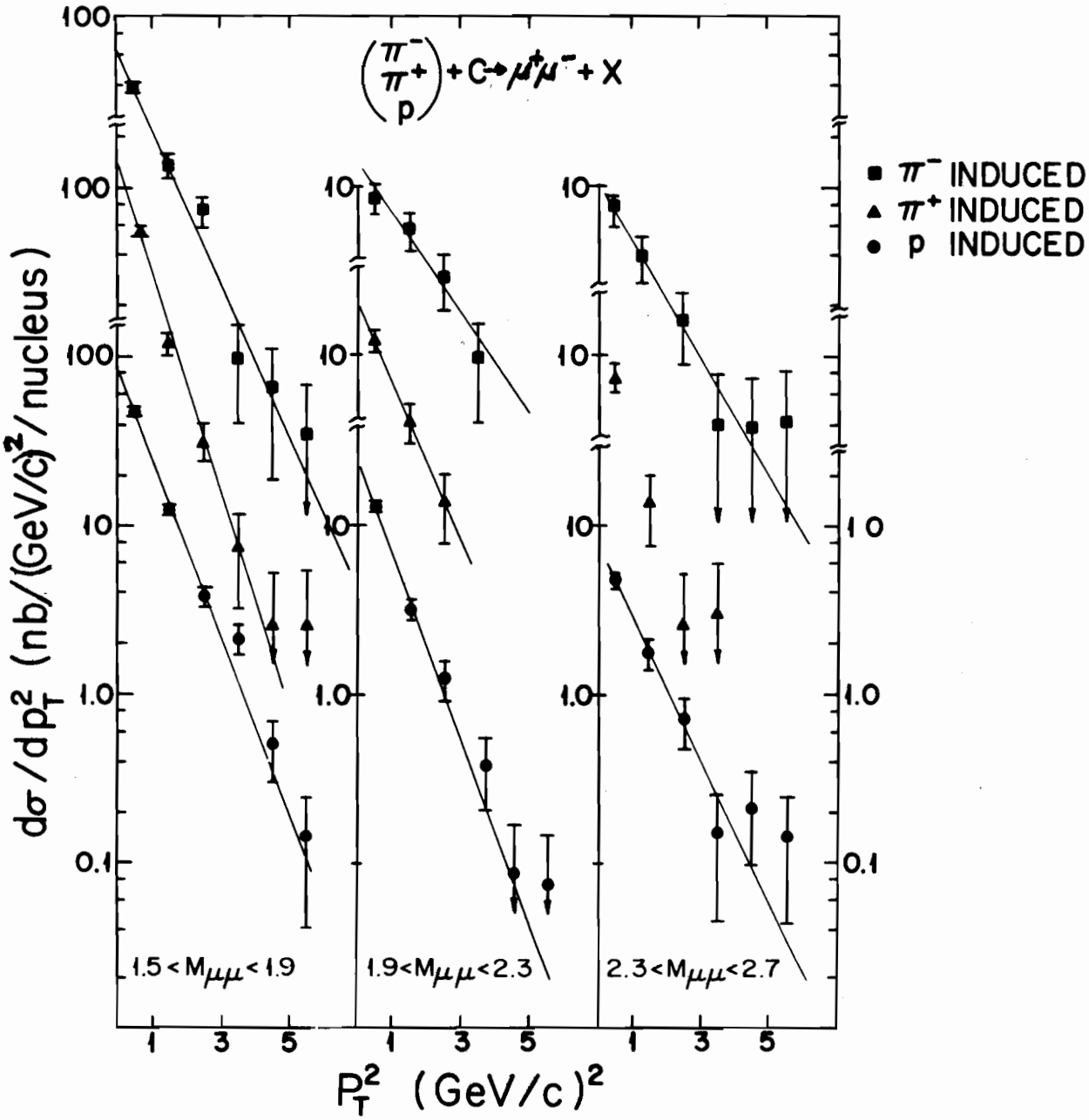
$\begin{pmatrix}\pi^- \\ \pi^+ \\ p\end{pmatrix}$ + C → $\mu^+\mu^-$ + X
■ π^- INDUCED
▲ π^+ INDUCED
● p INDUCED
$d\sigma/dp_T^2$ (nb/(GeV/c)^2/nucleus)
P_T^2 (GeV/c)^2
1.5 < Mμμ < 1.9
1.9 < Mμμ < 2.3
2.3 < Mμμ < 2.7

FIGURE 4

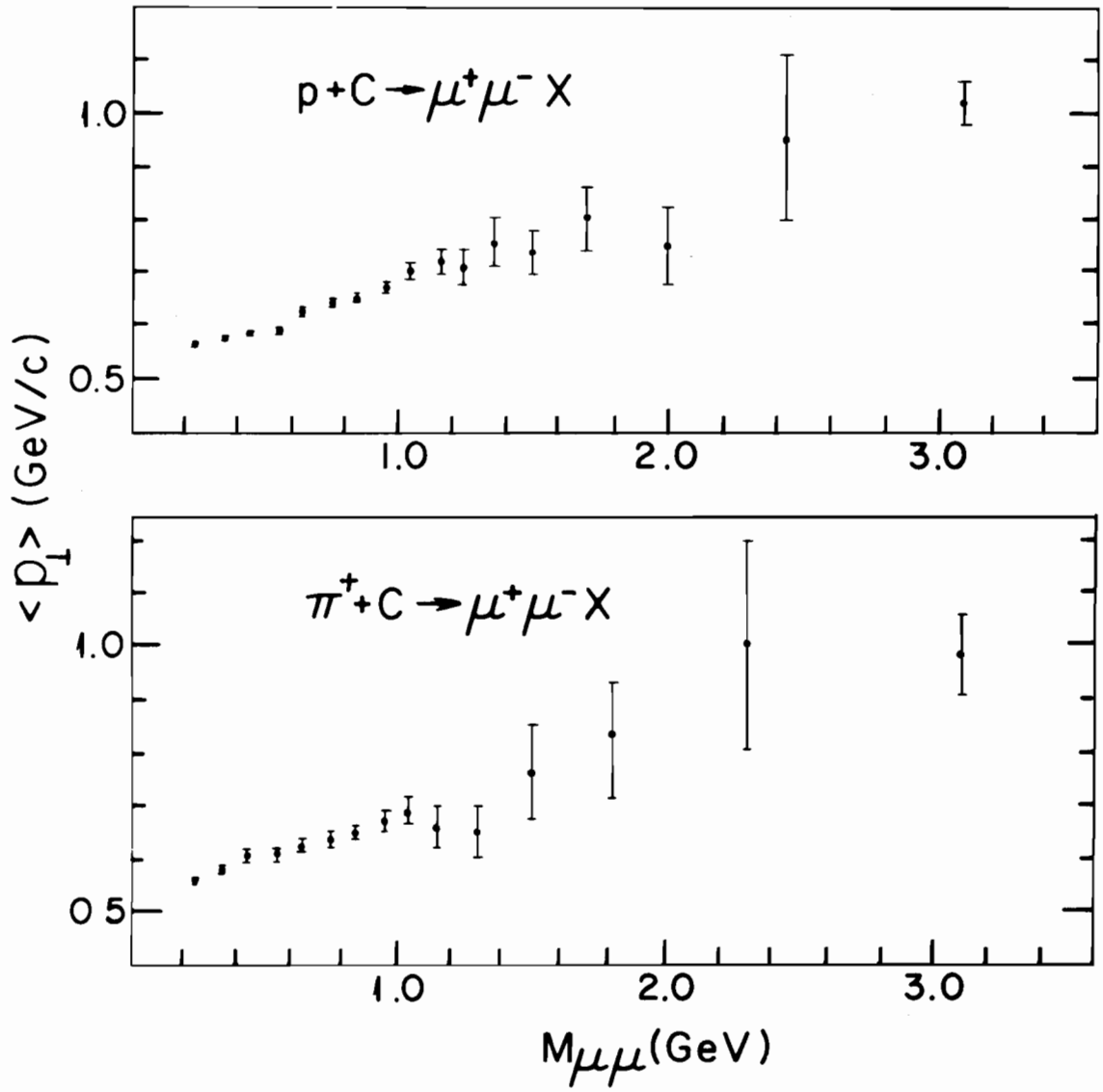

FIGURE 5

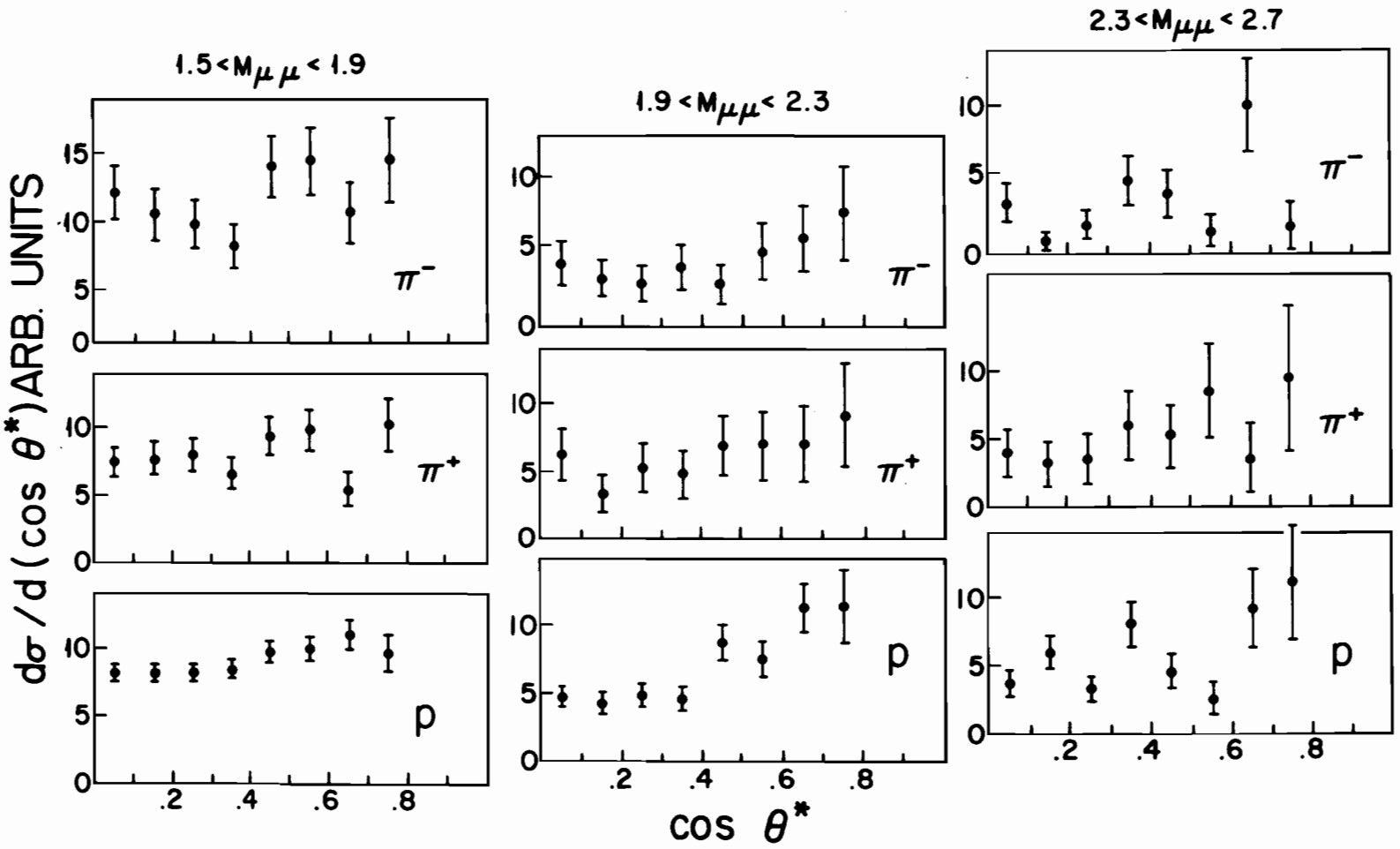

FIGURE 6

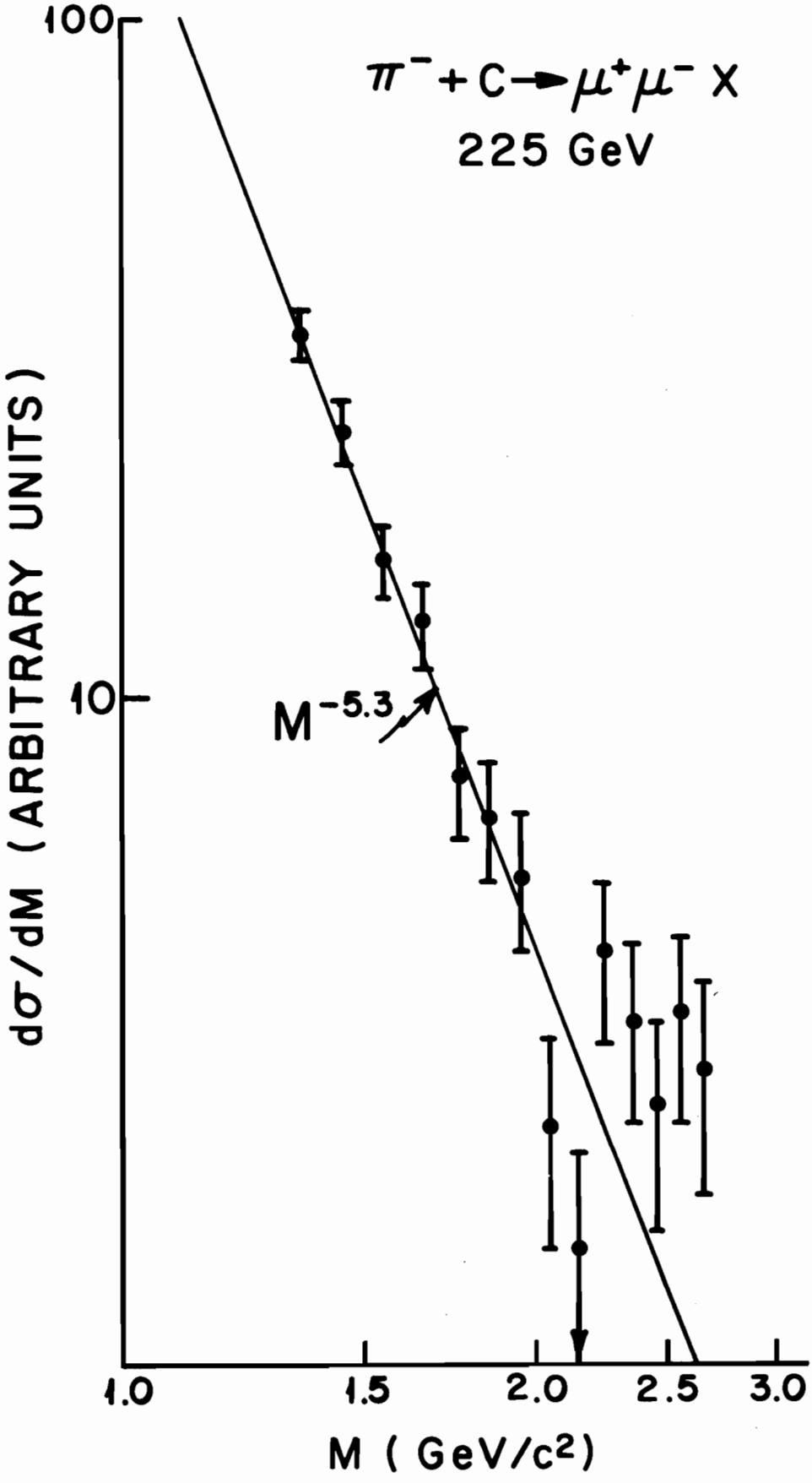
100
10
$\pi^- + C \rightarrow \mu^+\mu^- X$
225 GeV
$M^{-5.3}$
$d\sigma/dM$ (ARBITRARY UNITS)
1.0
1.5
2.0
2.5
3.0
M (GeV/c²)

FIGURE 7